



A generalized method for evaluating immediate post-earthquake losses of buildings from different perspectives

Shuang Li^{1,2} · Binbin Hu^{1,2} · Changhai Zhai^{1,2} · Paloma Pineda³

Received: 20 May 2024 / Accepted: 13 April 2025 / Published online: 7 May 2025
© The Author(s), under exclusive licence to Springer Nature B.V. 2025

Abstract

The evaluation of immediate post-earthquake losses of buildings is crucial for advancing resilience-based seismic design. To facilitate the development of resilient buildings, a generalized method suitable for any occupancy type of building is proposed to evaluate immediate post-earthquake losses of buildings from engineering, economic, and social perspectives. A functional composition diagram of the building story is constructed, and the story functionality is quantified by using the hierarchical belief rule base inference method based on the evidential reasoning algorithm. The functional composition diagram incorporates the service status of utility systems, such as power, water, communication, heating, and drainage networks, to reflect their impact on the story functionality. Intra-story damage relevance and inter-story functionality relevance of the building are also considered in the functional loss evaluation. To evaluate direct economic loss, two methods for calculating the repair cost ratio are proposed. The choice of method hinges on the level of detail available. Direct social loss is quantified in terms of the casualty ratio, with considerations for the varying impacts of different casualty severity levels on society. Applying this generalized method to a teaching building, the results show that the functional loss is more severe compared to the direct economic and social losses. From the perspective of resilience-based seismic design, it is essential to focus on mitigating functional losses of buildings. This method can provide guidance for pre-earthquake strengthening efforts and post-earthquake recovery strategies for buildings and contribute to advancing resilience-based seismic design.

Keywords Functional loss · Direct economic loss · Direct social loss · Belief rule base · Resilience-based seismic design

✉ Binbin Hu
binbinhu@stu.hit.edu.cn

¹ Key Lab of Structures Dynamic Behavior and Control of the Ministry of Education, Harbin Institute of Technology, Harbin 150090, China

² Key Lab of Smart Prevention and Mitigation of Civil Engineering Disasters of the Ministry of Industry and Information Technology, Harbin Institute of Technology, Harbin 150090, China

³ Department of Building Structures and Geotechnical Engineering, Universidad de Sevilla, Avda. Reina Mercedes, No. 2, Seville 41012, Spain

1 Introduction

Earthquakes are universally recognized as profoundly destructive natural disasters, resulting in extensive damage to facilities, substantial economic ramifications, and heavy casualties, thereby impeding urban development (Kitayama et al. 2023; Li et al. 2023; Sagbas et al. 2024). A notable example is the 2008 Wenchuan earthquake in China, which led to economic losses totaling \$130 billion and 69,000 fatalities (Li et al. 2021). The subsequent reconstruction efforts continued for three years. In Europe, there are also examples of destructive earthquakes that have caused significant losses both in the built environment and casualties; for instance, the 2009 L'Aquila earthquake in Italy, with 308 dead, 67,500 homeless, and dramatic damages in heritage buildings (D'Ayala and Paganoni 2011), or the 2011 Lorca earthquake in Spain, with 9 dead, more than 300 injured, and about \$1.078 billion in economic losses (Martínez-Cuevas and Gaspar-Escribano 2016). Additionally, earthquakes have the potential to trigger secondary disasters like landslides, mudslides, fires, nuclear incidents, and tsunamis (Zhou et al. 2020; Kamata et al. 2022). The devastating aftermath of an earthquake can also leave lasting psychological trauma on affected residents that proves difficult to heal. Concern over potential earthquake-related disasters has escalated due to advancements in science and technology, rapid urbanization, population concentration, and wealth accumulation.

Seismic resilience has emerged as a prominent study field in earthquake engineering, offering valuable insights into disaster prevention and mitigation. Several countries have set forth development objectives and strategic plans, such as the United States' National Earthquake Resilience, Japan's Fundamental Plan for National Resilience, and China's Resilient Urban and Rural Program (United Nations 2015; Zhai et al. 2024). The European Commission (EC) has established seismic resilience as a main goal within civil protection; moreover, the EC is promoting the development of policies and strategies that combine both seismic resilience and energy efficiency by means of sustainable retrofitting works in the built environment (Menna et al. 2022). Seismic resilience refers to an engineering system's ability to either maintain or quickly recover its functional state when hit by an earthquake (Bruneau et al. 2003; González et al. 2020). An engineering system with enhanced seismic resilience not only ensures the safety of individuals but also experiences fewer losses and achieves quicker recovery. Evaluating the post-earthquake losses of a system is an essential aspect of seismic resilience. Given that buildings serve as vital components of urban areas, examining the losses they endure following an earthquake holds paramount importance. A prompt and quantitative evaluation of post-earthquake losses would provide timely scientific guidance for post-earthquake emergency rescue and recovery efforts. Additionally, it would pave the way for the development of resilience-based seismic design.

In the context of community buildings, post-earthquake losses encompass various dimensions, including engineering, economic, and social aspects. These dimensions can be delineated by functional losses, repair costs, and casualties, respectively. Functional losses refer to the reduction in building functionality due to damage to its structural systems, non-structural systems, and contents. It is pertinent to note that current studies frequently concentrate on specific aspects of these losses rather than considering the various dimensions.

Hassan et al. (2018) allocated the total building losses obtained by referring to FEMA P-58-1 (FEMA 2018a) and HAZUS-MH5.1 (FEMA 2022) to each bottom component of the fault tree, which was used to describe the logical membership relationships of hospital

components. Then, the functionality was evaluated using the fault tree method. However, this process revealed logical flaws as it was deemed unreasonable to allocate component losses based on the total building losses. Shang et al. (2020) developed a healthcare system model and evaluated the hospital functionality and seismic resilience based on the state tree method by defining the healthcare system functional indicators and identifying the critical infrastructure and essential components that support the healthcare system functions. Terzic et al. (2021) and Terzic and Villanueva (2021) proposed a probabilistic post-earthquake functional evaluation method for buildings. They used the functionally restricted area within the building as an indicator of functional loss. Fault trees were established to capture the relationships between the functionalities of the building systems and individual components. Jiang et al. (2022) proposed a component assembly method to quantify the functional loss of a building. They added the functional loss as a new component loss function to the existing building component vulnerability data structure. The fuzzy theory was then employed, utilizing a logic tree to coordinate the functional loss of each component in a story. Qu et al. (2020) proposed a five-level functional framework for quantifying the functional losses of buildings during disasters. The building functionality was determined by a functionally weighted average of the sub-functions, with weighting factors reflecting the relative importance of the individual subsystems. Lu et al. (2022) defined building functionality as the weighted average of the functionalities of structural, architectural, and service components. The functional contribution of each type of component to the building was determined by structural engineers, who assigned appropriate weights accordingly.

There are many methods available to evaluate the economic and social losses of buildings. One such method is the Performance-Based Earthquake Engineering (PBEE) framework (Tesfamariam and Goda 2015). This framework has been used for the loss estimation of reinforced concrete and steel buildings that suffered earthquakes (Song et al. 2016; Cook et al. 2021). Dhakal and Mander (2005) expanded the PBEE framework by incorporating time, resulting in a quadruple integral formulation. Melani et al. (2016) used this quadruple integral formulation to estimate the expected annual loss of reinforced concrete structures by drawing fragility curves for different damage states of buildings. Wen et al. (2019) measured the post-earthquake economic loss using the economic loss ratio. HAZUS-MH5.1 (FEMA 2022) evaluated economic and social losses based on component fragility and consequence functions. Hassan et al. (2018) developed a method to estimate post-earthquake casualties of steel hospitals, considering factors such as indoor and outdoor occupant distribution as well as the timing of earthquakes. Additionally, some rating systems define resilience ratings for buildings of interest and explicitly state the relationships between ratings and repair costs and casualties (Almufti and Willford 2013; USCR 2017; GB/T 38591–2020 2020). These methods and frameworks offer useful tools for evaluating and quantifying the economic and social losses of buildings subjected to earthquakes.

The mentioned research indicates that there are two main categories of methods for evaluating post-earthquake functional loss. The first category uses fault tree analysis in conjunction with probability to evaluate functional loss. The second category involves calculating a weighted average of the functionality of different subsystems within a building. While both methods incorporate the idea of functional assembly, the weighted average method may not fully address the intricate dependencies among building systems. In contrast, fault trees offer a framework for multi-performance group functional assembly, making them well-suited for post-earthquake functional evaluation. However, fault trees are predominantly

used for evaluating hospital functionality, and an additional physical parameter needs to be introduced as a building functional indicator. Consequently, even if the same fault tree model is adopted, variations in functional evaluation results may occur due to differences in the definition of functional indicators. Although Jiang et al. (2022) proposed a generalized method for post-earthquake functional evaluation, they did not consider either the variability of building occupancy types or the service status of the external utility systems. In terms of estimating economic and social losses, methods are mainly derived from the PBEE framework, HAZUS-MH5.1 (FEMA 2022), and some rating systems (Almufti and Willford 2013; USCR 2017; GB/T 38591–2020 2020).

This study presents a generalized method for evaluating immediate post-earthquake losses of buildings from engineering, economic, and social perspectives.¹ The evaluation process is shown in Fig. 1, and the key components involved are summarized in Fig. 2. The functional loss is evaluated using a hierarchical belief rule base inference method based on the evidential reasoning algorithm (BRBI-ER), considering various functional characteristics of different occupancy types of buildings as well as intra-story damage relevance, inter-story functionality relevance, and the service status of external utility systems. Calculation processes are established for estimating direct economic loss and direct social loss based on HAZUS-MH5.1 (FEMA 2022) and rating system (GB/T 38591–2020 2020). The generalized method holds significant practical value. It can serve as a foundation for evaluating post-earthquake losses of building portfolios, offering valuable insights for pre-earthquake strengthening efforts and post-earthquake recovery decision-making. Furthermore, it contributes to the advancement of resilience-based seismic design, with a focus on strategies for mitigating post-earthquake losses.

2 Immediate post-earthquake losses of buildings

2.1 Building function classification

When evaluating or estimating post-earthquake losses, it is essential to classify buildings, as different types of buildings exhibit varying levels of vulnerability. Comprehensive classifications of buildings have been offered by HAZUS-MH5.1 (FEMA 2022). The classifications consider factors such as building materials, occupancy types, and structural types, allowing for a more precise estimation of potential damage and losses during seismic events. During the seismic risk assessment period from 1982 to 1985 in California, the Applied Technology Committee (ATC) found that while two facilities have similar structural types, the differences in engineering, economic, and social losses resulting from their different uses can be significant. To address this, ATC-13 (ATC 1985) has classified facilities into 78 types, including 40 building types. While these classifications are detailed, they are primarily tailored to American buildings and may not fully reflect the structural characteristics and uses of buildings in China. Consequently, directly applying the existing building classifications to Chinese buildings, which have unique localization features, presents a challenge. The authors have created classifications for the occupancy types of building drawing upon

¹Immediate post-earthquake losses describe losses occurring instantaneously after an earthquake, including functional, direct economic, and direct social losses. In contrast, direct losses generally denote economic and social losses directly induced by the seismic event.

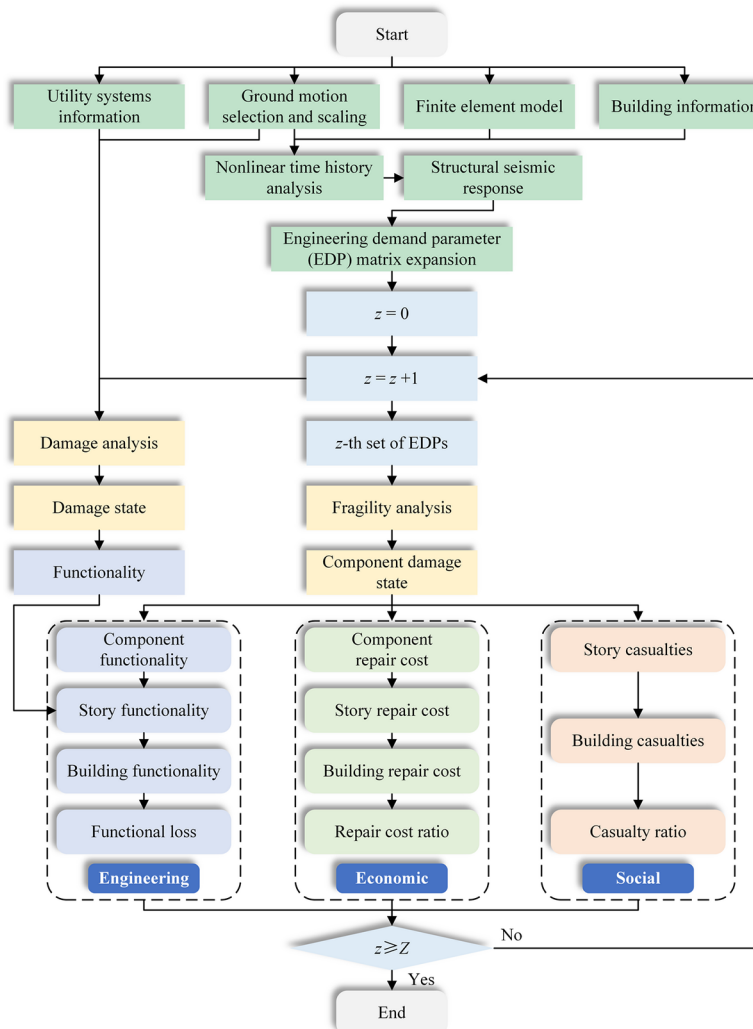


Fig. 1 The evaluation process

China's pertinent urban land use code (GB 50137–2011 2011) and on-site surveys (Li et al. 2024). Subsequent investigations have led to the enhancement of the previous classifications, as shown in the improved Table 1. Other countries may also reference or adapt this classification.

2.2 Functional loss

The functional loss of a building is calculated by subtracting the residual functionality from the pre-earthquake functionality. The residual functionality is derived by assembling the functionalities of all stories, categorized according to Table 1, to reflect their different uses. To evaluate the functionality of each story, a functional composition diagram, informed by

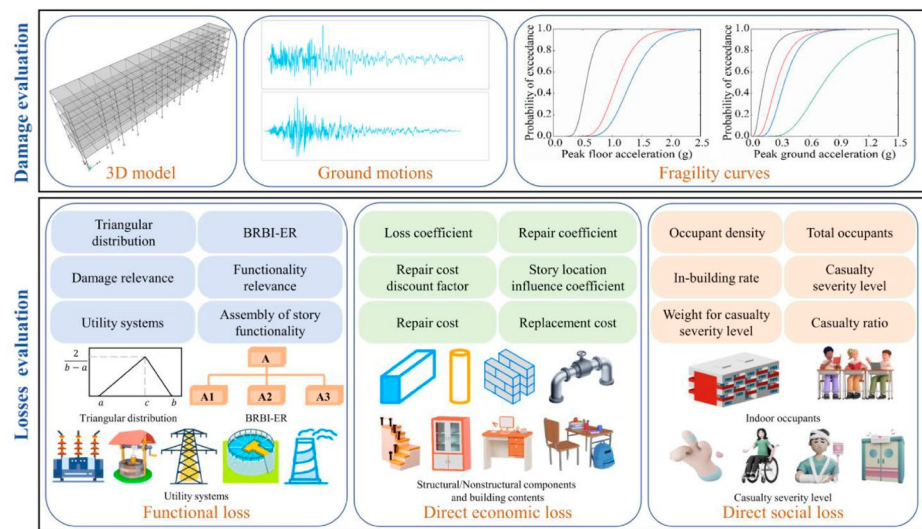


Fig. 2 Key components in this study

field investigations and existing research (Porter and Ramer 2012; Qu et al. 2020; Shang et al. 2020; Terzic et al. 2021), is constructed to delineate the relationships between building components and story function. BRBI-ER is adopted to infer story functionality from component functionality, with component functionality evaluated based on its damage state, determined through fragility analysis. The method enables the quick identification of components that impair building functionality.

2.2.1 Functional composition for story

Figure 3 shows a typical functional composition diagram for a story, categorizing its function into basic and advanced functions. The basic function pertains to the story's ability to withstand seismic effects, reduce casualties, and provide essential living conditions such as enclosure, lighting, water supply, and drainage. On the other hand, the advanced function arises from the story's specific attributes, such as residence, office, hospital, and education (Table 1). The basic function comprises component functions from both structural and non-structural systems. Nonstructural systems include space enclosure systems, vertical transportation, and accessory systems, in which the functions of the accessory systems reflect the functional dependencies between different systems. For example, the power system impacts the normal operation of the heating ventilation and air conditioning (HVAC) system and lighting system. It should be noted that the implementation of the advanced function often necessitates the support of components in the basic function. Additionally, different occupancy types of buildings demonstrate diverse preferences toward basic and advanced functions. For example, high-speed railway stations pay more attention to their advanced functions, specifically passenger transportation and freight transportation functions (Tang et al. 2023). In such cases, the basic function may be omitted, and only the functional composition diagram of the advanced function is established. Conversely, there may be instances where the advanced function takes a backseat and the focus is solely on the basic func-

Table 1 The classification of building occupancy types (Li et al. 2024)

Functional category	Occupancy type	Type descriptions
Residential	Single-family dwelling	Residential buildings that accommodate only one family
	Multi-family dwelling	Residential buildings that accommodate multiple families
	Institutional dormitory	Housing shared by employees or students
Public administration and service	Administrative office	Office buildings for social management
	Medical and health care	Hospitals and clinics that provide treatment for diseases and undertake public health prevention
	Transportation site	Stations, and other public buildings that provide transportation services
	Other services	Fire stations, communication buildings, and other public service buildings
Others	Scientific and educational building	Buildings for scientific research, education and teaching
	Cultural and recreational building	Buildings that provide public recreation and culture such as theaters, cinemas, concert halls, libraries, cultural centers, museums, exhibition halls, gymnasiums
	Memorial building	Gardens, temples, cemeteries and similar buildings
	Other buildings	Other buildings with public nature apart from mentioned
Commercial service	Shopping mall	Buildings that offer daily necessities and production materials
	Commercial service	Buildings that provide services such as leisure, rest and food
	Commercial office	Buildings where financial transactions can be conducted or for business management
Productive logistic	Productive building	Buildings that can make products
	Logistics building	Buildings that are the transfer centers of goods
	Warehousing building	Buildings used for storage of goods

tion. The functional composition diagram can be easily customized or adjusted for specific buildings as needed. Components unrelated to the building of interest can be removed, and supplementary components can be added to establish more detailed logical relationships regarding story function.

Damage to external utility systems may reduce building functionality. For example, a disruption in the external power supply can affect all electricity-dependent components within the building. Figure 3 incorporates the impacts of the service status of utility systems on maintaining the building's original functionality. Figure 4 provides a clearer overview of the utility systems examined. Utility components are simplified, as some may not suffer severe damage during earthquakes, or rather do not experience damage that hampers normal operation. Specifically, the focus is on substations and transmission and distribution lines for the power network; wells and water supply pipelines for the water network; central offices and communication towers for the communication network; drainage pumping stations and drainage pipelines for the drainage network; heating pump stations and heating supply pipelines for the heating network. While the analysis considers only partial com-

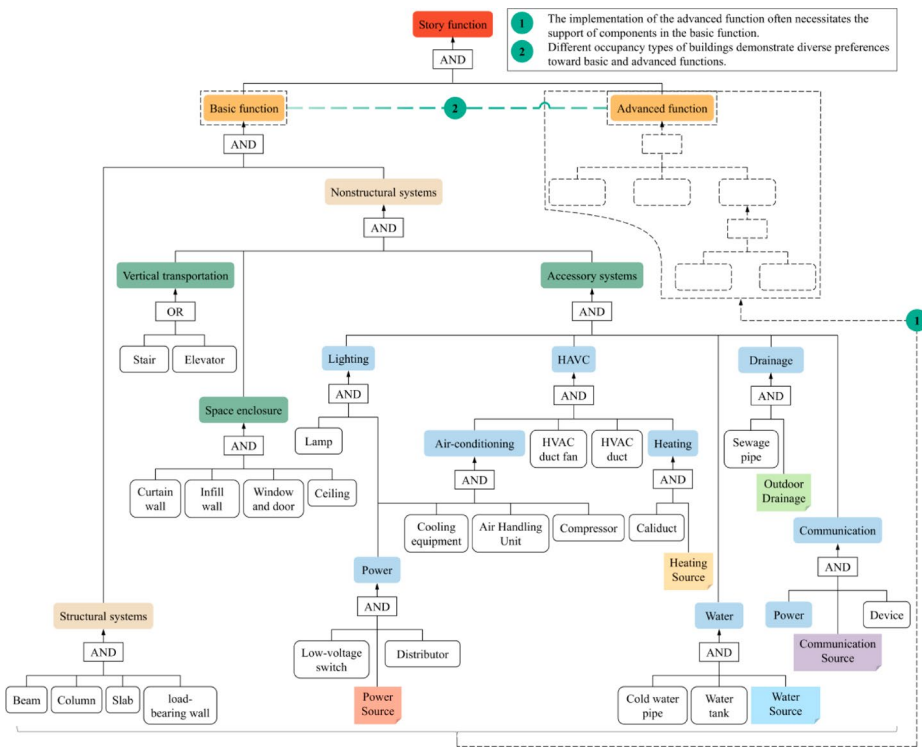
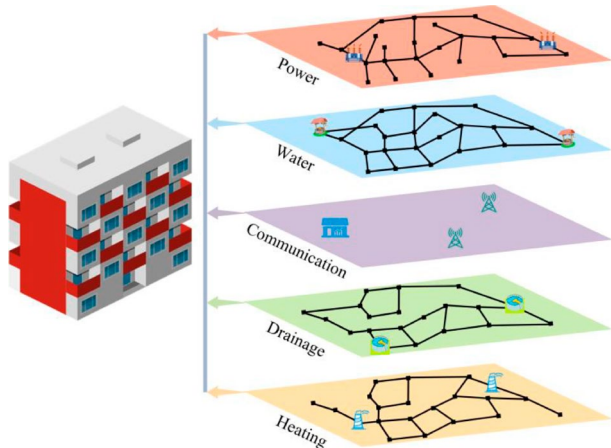


Fig. 3 Functional composition diagram for a story

Fig. 4 Utility systems serving for buildings



ponents of each utility system, it effectively demonstrates the impact of utility systems on building functionality. It is worth noting that more detailed and intricate assumptions can be made easily.

2.2.2 Component damage state

The PBEE framework provides a probabilistic methodology for assessing structural performance and guiding building design. It incorporates performance objectives, such as repair cost and repair time, that are important to decision-makers, stakeholders, and insurers. To enhance the practical implementation of PBEE, FEMA P-58-2 (FEMA 2018b) has created an extensive library covering over 700 structural and nonstructural building components, complete with fragility curves and associated consequence functions. Similarly, China has formulated a standard for assessing seismic resilience of buildings, which likewise involves a compilation of component fragility curves and consequence functions to estimate the repair cost, casualties, and repair time of buildings, thus assessing the resilience rating (GB/T 38591–2020 2020). Component fragility curves are essential in earthquake damage assessment and seismic resilience assessment, serving as a basis for quantifying losses in individual components and the overall building. The earthquake fragility analysis aims to estimate the probability of a component or structure reaching a specific damage state under different seismic intensity levels. Typically, the cumulative log-normal distribution function is utilized to establish a continuous function representing the component fragility, as shown in Eq. (1):

$$F_{dm}(x) = P[DM \geq dm|x] = \Phi\left(\frac{\ln(x/\alpha_{dm})}{\beta_{dm}}\right) \quad (1)$$

where $F_{dm}(x)$ is the fragility function; x is the earthquake intensity, which here refers to the EDPs or earthquake intensity measures (IMs); α_{dm} and β_{dm} are the median and standard deviation parameters, respectively, associated with the fragility curve; Φ is the standard normal cumulative distribution function.

When evaluating the damage states of building components, x signifies EDPs. A component usually has several damage states, each indicating different degrees of damage. The number of damage states varies for different components. For example, windows have two states, intact and broken, while ceilings could have four states. To denote damage states for components, the notation DS0, DS1, ..., DS n is adopted, where DS0 represents an intact state and DS n represents the most severe damage state. Actually, component damage may not solely result from the seismic excitation but can also be impacted by other components. Damage to an infill wall may lead to the damage or falling of objects attached to its surface, and severe peeling of slabs exacerbates damage to ceilings. Thus, there exists intra-story damage relevance among components. While there are no definitive earthquake damage statistics available to quantify damage relevance, this attempt may provide a more comprehensive consideration for damage evaluation.

The normalized damage states are defined as Eq. (2) to facilitate the calculation of the component functionality, which is described in detail in Sect. 2.2.3.

$$DSi = i/n \quad (2)$$

where $i=0, 1, 2, \dots, n$; $DSi \in [0, 1]$, DS0 is the normalized intact state; DS1 is the normalized state with the most severe damage.

Based on the seismic intensity levels, the IMs are determined. After obtaining the parameters, the damage states of utility systems can be evaluated. The damage model for pipelines is characterized by a Poisson distribution to estimate the probability of n damages occurring for a given pipeline (Gehl et al. 2021):

$$P(n) = \frac{(RR \cdot L)^n}{n!} \cdot e^{-RR \cdot L} \quad (3)$$

where $P(n)$ is the probability of experiencing n damages in a pipeline; RR is the repair rate under the same peak ground velocity (PGV), which represents the average number of repairs required per unit length; L is the length of the pipeline. The repair rate can be estimated as follows:

$$RR = 0.0001 \times \text{PGV}^{2.25} \quad (4)$$

where PGV is measured in cm/s.

The damage states of utility components other than pipelines are evaluated based on the fragility function, where x represents the IM, which is peak ground acceleration (PGA) here. The normalized expression is also employed to represent the damage states.

2.2.3 Component functionality

Many agents, including engineers and stakeholders, contend that the functional degradation of a building exposed to an earthquake is reliant on the residual functionalities of its components. Dong and Frangopol (2016) suggested that the residual functionality of a component under different damage states can be estimated using a triangular distribution. It has been observed that as the severity of component damage escalates, the residual functionality diminishes. To simplify, the median parameter of the triangular distribution is assumed to be linearly correlated with the damage state:

$$Q_{r,\text{med}} = 1 - \text{DS}_i \quad (5)$$

where $Q_{r,\text{med}}$ is the median parameter of the triangular distribution.

Based on HAZUS-MH5.1 (FEMA 2022), the residual functionality of a pipeline can be characterized by the serviceability index, as shown in Eq. (6):

$$SI = 1 - \Phi \left(\frac{\ln(\overline{RR}/\alpha_{\overline{RR}})}{\beta_{\overline{RR}}} \right) \quad (6)$$

where SI is the serviceability index; \overline{RR} is the average repair rate of all pipelines under different PGVs; $\alpha_{\overline{RR}}$ is the median of the average repair rate; $\beta_{\overline{RR}}$ is the standard deviation of the average repair rate.

The residual functionality of utility components, excluding pipelines, is also similarly adhered to a triangular distribution. Given the interconnected nature of external utility components, it is posited that these components are in a series relationship, and the residual functionality of each utility system is dictated by its component with the lower functional-

ity. For example, the residual functionality of the power network is taken as the smaller value of the residual functionalities of the substation and transmission and distribution lines. For building portfolios, a network topology relationship can be established between utility systems and buildings (Anwar et al. 2023). Functionality can be evaluated by connectivity analysis, user requirement analysis, etc.

2.2.4 Story functionality

After calculating the residual functionality of each component, BRBI-ER is employed to evaluate story functionality. BRBI-ER is a complex system modeling method that extends traditional D-S evidence theory, IF-THEN rules, and other basic theories (Tang et al. 2023). It can handle qualitative knowledge and quantitative data and establish nonlinear relationships between input and output variables to achieve derivation from component functionality to story functionality. BRBI-ER employs evidence reasoning for knowledge deduction, enabling the effective representation, transformation, and integration of uncertain input information to derive unified results.

BRBI-ER consists of two parts: knowledge expression and knowledge reasoning. Knowledge expression is achieved through the utilization of a belief rule base. By assigning belief degrees to the result section of the IF-THEN rule and considering both the antecedent attribute weights and rule weights, the belief rule can be established, as shown in Eq. (7). Putting a series of belief rules together forms a belief rule base.

$$R_k: \text{If } x_1 \text{ is } A_1^k \wedge x_2 \text{ is } A_2^k \wedge \cdots \wedge x_M \text{ is } A_M^k, \text{ Then } \{(D_1, \beta_{1,k}), (D_2, \beta_{2,k}), \dots, (D_N, \beta_{N,k})\} \quad (7)$$

With a rule weight θ_k and antecedent attribute weight $\delta_{1,k}, \delta_{2,k}, \dots, \delta_{M_k,k}$

where x_i ($i=1, 2, \dots, M_k$) is the antecedent attribute input; A_i^k is the reference value of the i th antecedent attribute in the k th rule; M_k is the number of antecedent attributes in the k th rule; θ_k is the rule weight of the k th rule; $\delta_{i,k}$ is the weight of the i th antecedent attribute in the k th rule; $\beta_{N,k}$ is the belief level of the N th evaluation result D_N in the k th rule relative to the output.

Knowledge reasoning is conducted by utilizing the evidential reasoning parsing algorithm, and the process can be described as follows:

Step1: determination of rule activation.

$$\omega_k = \frac{\theta_k \prod_{i=1}^{M_k} (\alpha_i^k)^{\bar{\delta}_{i,k}}}{\sum_{l=1}^L \theta_l \prod_{i=1}^{M_k} (\alpha_i^l)^{\bar{\delta}_{i,l}}} \quad (8)$$

$$\bar{\delta}_{i,k} = \frac{\delta_{i,k}}{\max_{i=1,2,\dots,M_k} \{\delta_{i,k}\}} \quad (9)$$

where α_i^k is the belief degree of x_i with respect to the referential value A_i^k for the k th rule; ω_k is the activation weight of the k th rule, which reflects the degree of agreement between the

rules and the input information; $\delta_{i,k}$ is the normalized weight of the i th antecedent attribute in the k th rule.

Step2: calculation of distributed results.

$$\mu = \left[\sum_{n=1}^N \prod_{k=1}^L (\omega_k \beta_{n,k} + 1 - \omega_k \sum_{n=1}^N \beta_{n,k}) - (N-1) \prod_{k=1}^L (1 - \omega_k \sum_{n=1}^N \beta_{n,k}) \right]^{-1} \quad (10)$$

$$\beta_n = \frac{\mu \left[\prod_{k=1}^L (\omega_k \beta_{n,k} + 1 - \omega_k \sum_{n=1}^N \beta_{n,k}) - \prod_{k=1}^L (1 - \omega_k \sum_{n=1}^N \beta_{n,k}) \right]}{1 - \mu \left[\prod_{k=1}^L (1 - \omega_k) \right]} \quad (11)$$

$$S(x) = \{(D_n, \beta_n), n = 1, 2, \dots, N\} \quad (12)$$

where μ is the normalization factor; $S(x)$ is the distributed output result.

Step3: estimation of single-point result.

$$\hat{y} = \sum_{n=1}^N \mu(D_n) \beta_n \quad (13)$$

where \hat{y} is the estimated value.

Based on the functional composition of a story as illustrated in Fig. 2, belief rule bases are established. Taking the residual functionality of components as inputs, Eqs. (8) - (13) are used to sequentially infer upper-level functionalities in a bottom-up manner. The story functionality is ultimately derived as the culmination of this hierarchical inference process.

To illustrate the application of BRBI-ER, a concise example is presented. Suppose that after multiple inferences, the basic function and advanced function in Fig. 2 are derived, with their respective functionalities determined as 0.48 and 0.84. These functionalities are then utilized as input data to infer the story functionality. Each data is characterized by three reference states: *full*, *half*, and *none*. Based on empirical investigations and domain expertise, a rule base is established (Table 2). Prior to inference, it is necessary to convert the input data into a distributed form using Eqs. (14)-(16):

$$\begin{cases} \beta_{half} = (\gamma_{full} - x_i) / (\gamma_{full} - \gamma_{half}) \\ \beta_{full} = 1 - \beta_{half} \\ \beta_{none} = 0 \end{cases} \quad \gamma_{half} < x_i \leq \gamma_{full} \quad (14)$$

$$\begin{cases} \beta_{none} = (\gamma_{half} - x_i) / (\gamma_{half} - \gamma_{none}) \\ \beta_{half} = 1 - \alpha_{none} \\ \beta_{full} = 0 \end{cases} \quad \gamma_{none} \leq x_i \leq \gamma_{half} \quad (15)$$

$$Z(x) = \{(full, \alpha_{full}), (half, \alpha_{half}), (none, \alpha_{none})\} \quad (16)$$

where γ_{full} is 1.0; γ_{half} is 0.5; γ_{none} is 0; $Z(x)$ is the distributed input data.

Table 2 The rule base for the illustrative example

Rule	IF	THEN
1	(B is full \wedge C is full)	A is {(full, 1)}
2	(B is half \wedge C is full)	A is {(full, 0.7), (half, 0.3)}
3	(B is none \wedge C is full)	A is {(none, 1)}
4	(B is full \wedge C is half)	A is {(full, 0.6), (half, 0.4)}
5	(B is half \wedge C is half)	A is {(half, 1)}
6	(B is none \wedge C is half)	A is {(none, 1)}
7	(B is full \wedge C is none)	A is {(full, 0.2), (half, 0.2), (none, 0.6)}
8	(B is half \wedge C is none)	A is {(half, 0.4), (none, 0.6)}
9	(B is none \wedge C is none)	A is {(none, 1)}

Note: A, B, and C represent basic functionality, advanced functionality and story functionality, respectively

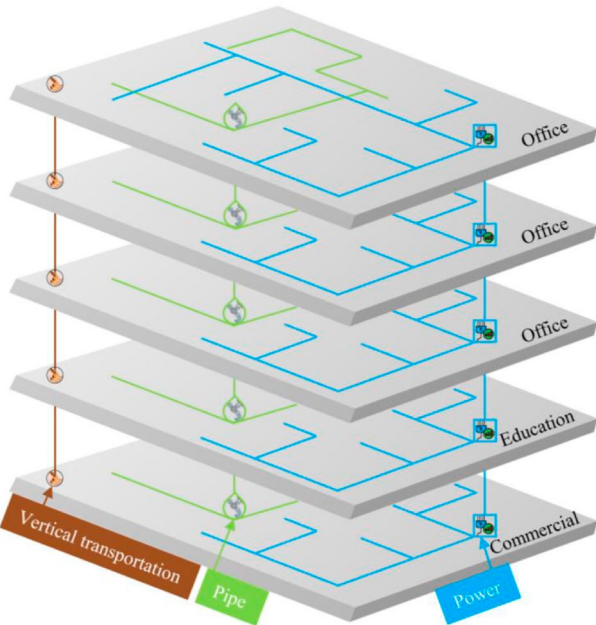
Assuming that all rule weights and antecedent attribute weights are 1. According to Eq. (8), the activation weights of 1~9 rules can be calculated, which are $w_1=0.1016$, $w_2=0.4821$, $w_3=0.1285$, $w_4=0.0205$, $w_5=0.0972$, $w_6=0.0259$, $w_7=0.0206$, $w_8=0.0976$, and $w_9=0.026$, respectively. The distributed evaluation result of story functionality is {(full, 0.5205), (half, 0.2975), (none, 0.1821)}, and the residual functionality is calculated to be 0.67 using Eq. (13).

2.2.5 Building functionality

The functionalities of all stories calculated through Sect. 2.2.4 are independent. In reality, the story functionality is not only related to components within that specific story but also to the components of the adjacent stories, especially components such as vertical transportation, power, and pipe systems that are continuously distributed along the height of buildings. These components create clear relevance among the functionalities of different stories, which is referred to as inter-story functionality relevance. The presence of functionality relevance increases the vulnerability of buildings. As depicted in Fig. 5, the functionality relevance of vertical transportation, power, and pipe systems is considered. Functionality relevance is closely related to the orientation of vertical components within buildings. Specifically, for vertical transportation, spatial flow generally progresses from lower stories to upper stories. Therefore, the functionality of vertical transportation in upper stories is represented by the functionality in lower stories. This principle similarly applies to power systems, which generally follow a bottom-to-top power distribution pattern. However, different definitions may apply to pipe systems. For water supply pipes that operate from top to bottom, the functionality of those located in lower stories is influenced by the operation of pipes in upper stories. Conversely, this relevance inverts when the water supply configuration operates from bottom to top. As for sewage pipes and caliducts, the functionality of upper-story pipes depends on the normal operation of lower-story pipes.

The building functionality is derived from the functionalities of individual stories, as illustrated in Eq. (17). This equation takes into account the influence of the occupancy type (Fig. 5) and the dimensional size of each story on the building functionality. Furthermore, it incorporates the extent of damage sustained by each story.

Fig. 5 Schematic on inter-story functionality relevance



$$Q = \frac{\sum_{f=1}^g \alpha_f \beta_f A_f Q_{s,f}}{\sum_{f=1}^g \alpha_f A_f} \quad (17)$$

where Q is the building functionality; $Q_{s,f}$ is the functionality of the f th story; A_f is the area of the f th story; α_f is the weighting factor corresponding to the occupancy type of the f th story; β_f is the impact coefficient indicating the influence of the f th story's damage state on the building functionality. β_f takes 1 if the story is intact, slightly damaged, or moderately damaged, and a value of 0 if the story or any story below is seriously damaged or in a worse state.

2.3 Direct economic loss

The estimation of direct economic loss of a building relies on the post-earthquake repair cost. To facilitate comparisons of direct economic losses across different regions, the repair cost ratio is used as an indicator. The repair cost ratio is defined as the ratio of repair cost to building replacement cost, as shown in Eq. (18):

$$\kappa = R_T / C_T \quad (18)$$

where κ is the repair cost ratio; R_T is the repair cost; C_T is the building replacement cost, which is the total cost required for constructing the target building according to current quotas.

Two different methods, Method A and Method B, are presented for estimating repair cost and building replacement cost. Method A requires detailed information about the building components, resulting in relatively accurate estimation results, while Method B provides slightly rougher estimates as it does not consider detailed building information. The two methods are described in turn below. The calculation process for Method A is illustrated using Eqs. (19) - (22).

$$R_{u,f} = \zeta_{C,u} \sum_{v=1}^V \eta_{1,u,v} C_{u,v,f} \eta_{2,u,v} \quad (19)$$

$$R_f = \sum_{u=1}^m R_{u,f} \quad (20)$$

$$R_T = \sum_{f=1}^g \lambda_{C,f} R_f \quad (21)$$

$$C_T = \sum_{u=1}^m C_u \quad (22)$$

where $\eta_{1,u,v}$ is the loss coefficient for the u -class component when it is in the damage state of v ; $\eta_{2,u,v}$ is the repair coefficient for the u -class component when it is in the damage state of v ; $C_{u,v,f}$ is the total cost of the u -class component when it is in the damage state of v within the f th story, calculated using current quotas; $\zeta_{C,u}$ is the repair cost discount factor that considers the amount of repair work for the u -class component; $R_{u,f}$ is the repair cost of the u -class component within the f th story; R_f is the repair cost of all components within the f th story; $\lambda_{C,f}$ is the coefficient that represents the influence of the story location on the repair cost; C_u is the construction cost of the u -class component calculated according to the current quotas.

Method B assumes that the direct economic loss consists primarily of the losses of the main structural systems, nonstructural components, and building contents. These losses are calculated based on the replacement cost of the main structural systems, as shown in Eqs. (23) - (27):

$$R_{s,f} = C_{s,f} \mu_{s,v,f} \quad (23)$$

$$R_{ns,f} = C_{s,f} \eta_{ns,f} \mu_{ns,v,f} \quad (24)$$

$$R_{in,f} = C_{s,f} \eta_{in,f} \mu_{in,v,f} \quad (25)$$

$$R_T = \sum_{f=1}^g (R_{s,f} + R_{ns,f} + R_{in,f}) \quad (26)$$

$$C_T = \sum_{f=1}^g (C_{s,f} + C_{s,f}\eta_{ns,f} + C_{s,f}\eta_{in,f}) \quad (27)$$

where $C_{s,f}$ is the replacement cost of the main structural systems of the f th story of the building, which can be determined according to the local market cost price; $R_{s,f}$, $R_{ns,f}$ and $R_{in,f}$ are the repair costs of the main structural systems, nonstructural components, and building contents within the f th story; $\eta_{ns,f}$ is the non-structure ratio, which refers to the ratio of the nonstructural replacement cost of the f th story of the building to the replacement cost of the main structural systems; $\eta_{in,f}$ is the building contents ratio, which refers to the ratio of building contents property value to the replacement cost of the main structural systems; $\mu_{s,v,f}$, $\mu_{ns,v,f}$ and $\mu_{in,v,f}$ are the structure loss ratio, non-structure loss ratio, and building contents loss ratio when the f th story of the building is in the damage state of v . The structure loss ratio refers to the ratio of the repair unit price of the main structural systems to their replacement unit price; the non-structure loss ratio refers to the ratio of the repair cost of the non-structural components to their total replacement cost; the building contents loss ratio refers to the ratio of the building contents property loss to their total value. The non-structure ratio and the building contents ratio are known to be closely related to the occupancy type of the building. The structure loss ratio, non-structure loss ratio, and building contents loss ratio are influenced by the structural type of the building.

2.4 Direct social loss

Direct social loss resulting from an earthquake can be quantified by the casualty ratio, which is defined as the ratio of the number of casualties in the building to the total number of occupants (Eq. (28)). The casualty severity can be categorized into four levels according to RISN-TG041-2022 (2022), ranging from level 1 for basic medical aid requirements to level 4 for immediate death or death after treatment. The number of casualties in an earthquake is closely associated with the timing of the event. If an earthquake occurs at night, when most people are indoors and potentially asleep, the reaction time may be longer, leading to a higher number of casualties. Conversely, if the earthquake occurs during commuting hours when many people are outdoors or on transport, the number of casualties is likely to be lower. Therefore, evaluating casualties requires considering the in-building rate at different times. The casualty ratio can be calculated using Eqs. (28) - (31).

$$\gamma_{ID} = M_{ID}/P \quad (28)$$

$$P = \sum_{f=1}^g \zeta_f A_f \quad (29)$$

$$P_{in} = \sum_{f=1}^g \zeta_f A_f \xi_f \quad (30)$$

$$M_{ID} = \sum_{l=1}^4 \lambda_l \alpha_l P_{in} \quad (31)$$

where γ_{ID} is the casualty ratio; M_{ID} is the number of casualties; P is the total number of occupants; P_{in} is the number of indoor occupants; ζ_f is the occupant density of the f th story, measured in occupant per square meter ($\text{occupant}/\text{m}^2$), which is closely related to the occupancy type of the story; ξ_f is the in-building rate of the f th story, which is between 0 and 1, indicating the proportion of occupants who are indoors during the specified time period; α_l is the casualty rate for different casualty severity levels, ranging from level 1 to level 4, as mentioned earlier; λ_l is the weight assigned to each casualty severity level, emphasizing that different severity levels have different impacts on society.

3 Case study

3.1 Building information

To illustrate the proposed method, a case study is carried out on a five-story teaching building designed in compliance with the current Chinese seismic design code (GB50011-2010 2010). This building features a reinforced concrete frame structure, a widely used structural form for teaching buildings. The structural layout and reinforcement details are shown in Fig. 6, where columns with different reinforcement configurations are distinguished by color, and beams are distinguished by the orientation of two axis labels. The height of the first story is 4.2 m, while the subsequent stories are 3.6 m. The building is designed to with-

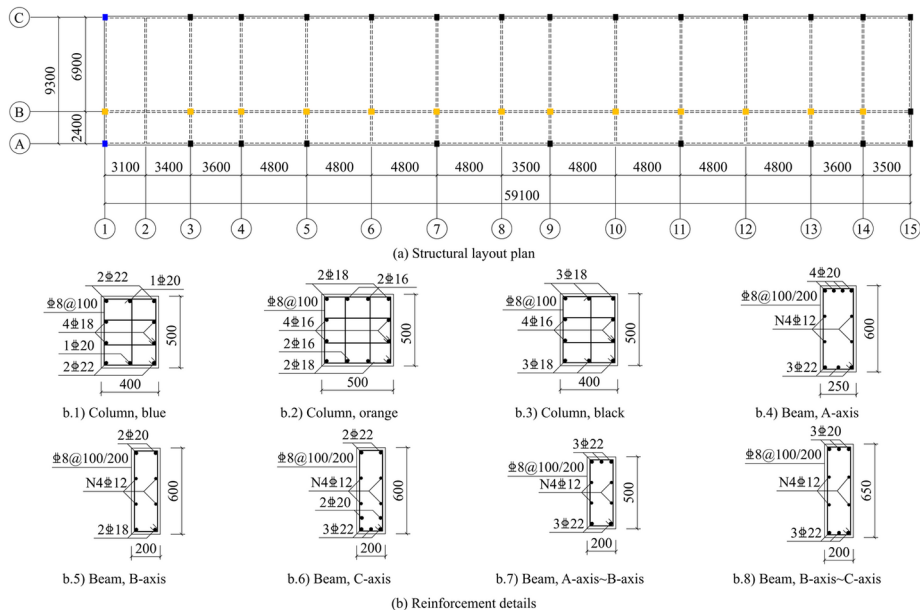


Fig. 6 Structural layout plan and reinforcement details

stand a seismic fortification intensity of 8 and is situated on Class II soil. The internal layout of the teaching building is presented in Fig. 7, showcasing the functional arrangement of various rooms. The layouts of the second, third, and fourth stories are identical. The teaching function is considered as the advanced function, and its functional composition diagram is shown in Fig. 8. Table 3 lists the 35 component types considered in this case study. When using BRBI-ER to infer upper-level functionalities, components 1–5, 7–8, 16–20, 22–24, and 26 have three reference states: *full*, *half*, and *none*, while all other components have two reference states: *full* and *none*. Cold water pipes supply water from top to bottom in this teaching building, with the functionality of those in lower stories being influenced by the operation of pipes in upper stories. The water source, outdoor drainage, and heating source are conveyed through pipelines of 6 km, 8 km, and 10 km to serve the teaching building, respectively.

3.2 Seismic responses

The proposed evaluation method requires the calculation of the seismic responses of the teaching building. This building model is developed using the material library and element

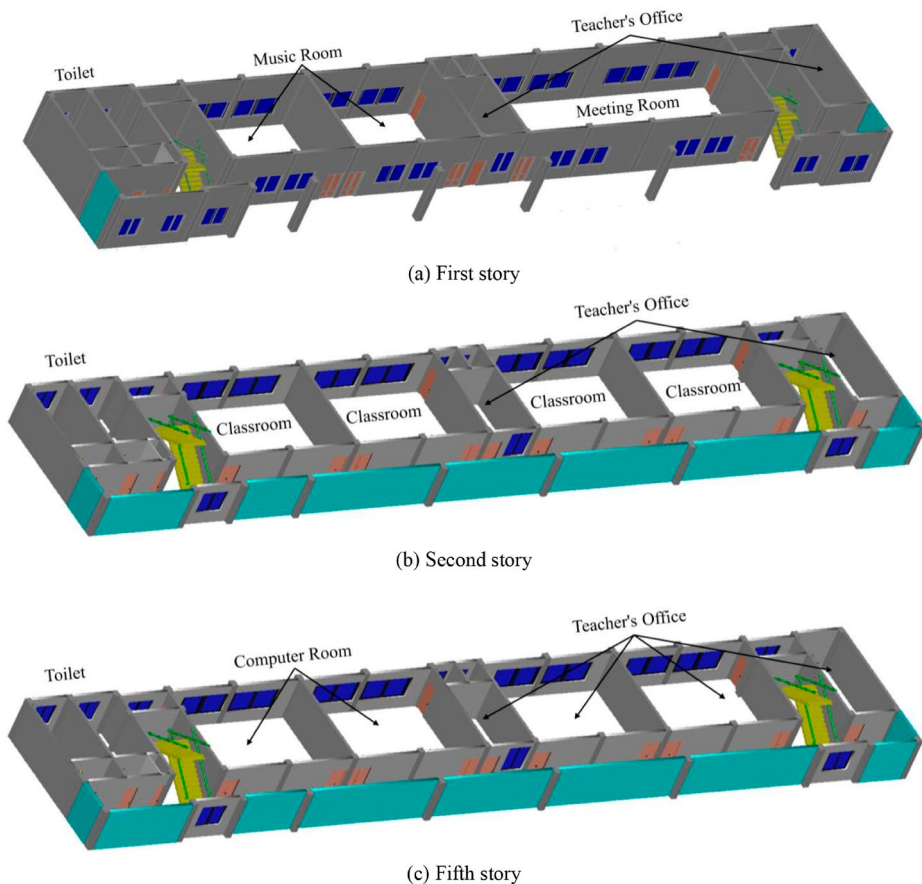


Fig. 7 Internal room layout plan

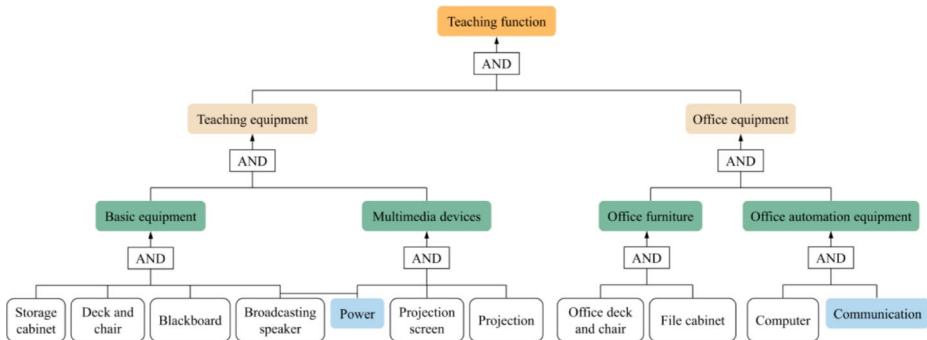


Fig. 8 Teaching function composition diagram

library in OpenSees (McKenna et al. 2000). For the concrete elements, a C30 designation is used, with an elastic modulus of 30GPa and an average axial compressive strength of concrete at 26.7MPa. The steel bars have an elastic modulus of 200GPa and an average yield strength of 443.8MPa. The concrete material is represented using the uniaxial Kent-Scott-Park model (Concrete01), which does not consider tensile strength but accounts for the confinement effect of hoops on the concrete. The steel bar material follows the uniaxial Giuffré-Mengotto-Pinto model (Steel02) with a strain hardening coefficient of 0.01, and default values control the transition from elastic to plastic curves. Beam and column elements are simulated using fiber section, where steel bars are positioned and distributed within the fibers based on their actual locations. However, the fiber section does not account for shear and torsion effects. To address this, the section aggregator is used to supplement the definition of shear and torsional stiffness for the section. Displacement-Based Beam-Column elements are employed to simulate the nonlinear behavior of beam and column components under seismic excitation. Each element is divided into five cross-sectional integral points to capture the response accurately. The structural analysis considers the distribution of actual constant and live loads, as well as $P\text{-}A$ second-order effects. The damping ratio of the building is set at 5% to account for energy dissipation during seismic events.

From the PEER ground motion database, thirteen ground motion records are selected on the basis of the following criteria: (1) seismic moment magnitude (M_w) ranging from 6.0 to 8.5; (2) epicenter distance (R_{jb}) falling within 0 to 45 km; (3) mean shear wave velocity of 30 m depth ($V_{s,30}$) ranging from 260 m/s to 510 m/s; and (4) a good match between the mean acceleration response spectrum of selected thirteen ground motions and the design response spectrum specified in the Chinese code (GB 50011–2010 2010). These ground motion records are detailed in Table 4. A comparison between the mean response spectrum (derived from the thirteen records) and the design response spectrum is shown in Fig. 9, demonstrating a favorable alignment between the two spectra. Intensity-based assessment is performed to evaluate the immediate post-earthquake losses of the teaching building across three seismic intensity levels: frequent earthquake (with a probability of occurrence exceeding 63.2% in 50 years, $\text{PGA}=0.07 \text{ g}$), basic earthquake (with a probability of occurrence exceeding 10% in 50 years, $\text{PGA}=0.2 \text{ g}$), and rare earthquake (with a probability of occurrence ranging from 2% to 3% in 50 years, $\text{PGA}=0.4 \text{ g}$). Figure 10 shows the peak inter-story drift ratio (PIDR) and peak floor acceleration (PFA) under different seismic intensity levels. The propagation and attenuation of ground motion are not considered, and it is assumed that

Table 3 Components considered in the teaching building

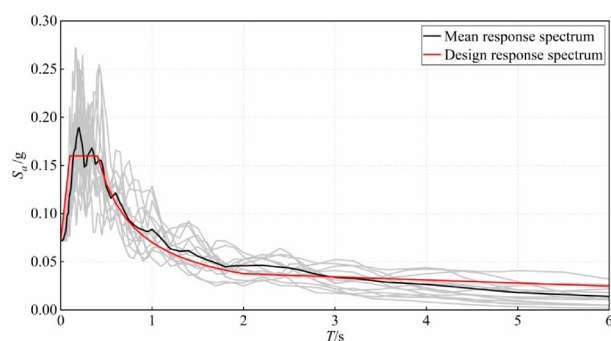
No.	Component	Story distribution	EDP/IM	α_{dm}	β_{dm}	Ref.	
1	Beam	1–5	PIDR	0.002	0.4	Cong 2022	
2	Column	1–5	PIDR	0.003	0.4	Cong 2022	
3	Slab	1–5	PIDR	0.01	0.25	FEMA 2018b	
4	Curtain wall	1–5	PIDR	0.026	0.25	GB/T 38591–2020 2020	
5	Infill wall	1–5	PIDR	0.005	0.4	GB/T 38591–2020 2020	
6	Window and door	1–5	PIDR	0.021	0.45	Shang 2021	
7	Ceiling	1	PFA	0.56 g	0.25 g	GB/T 38591–2020 2020	
8	Stair	1–5	PIDR	0.005	0.6	GB/T 38591–2020 2020	
9	Low-voltage switch	1–5	PFA	2.16 g	0.45 g	GB/T 38591–2020 2020	
10	Distributor	1–5	PFA	2.16 g	0.45 g	GB/T 38591–2020 2020	
11	Power source	Substation Transmission and distribution line	Outdoors Outdoors	PGA PGA	0.13 g 0.24 g	0.65 g 0.25 g	FEMA 2022 FEMA 2022
12	Lamp	1–5	PFA	0.56 g	0.25 g	GB/T 38591–2020 2020	
13	Cooling equipment	1–5	PFA	0.2 g	0.4 g	GB/T 38591–2020 2020	
14	Compressor	1–5	PFA	0.25 g	0.45 g	GB/T 38591–2020 2020	
15	Air handling unit	1–5	PFA	0.25 g	0.4 g	GB/T 38591–2020 2020	
16	Caliduct	1–5	PFA	0.55 g	0.5 g	GB/T 38591–2020 2020	
17	Heating source	Pump station Heating supply pipeline	Outdoors Outdoors	PGA PGV	0.13 g -	0.6 g -	FEMA 2022 -
18	HVAC duct fan	1–5	PFA	1.9 g	0.4 g	GB/T 38591–2020 2020	
19	HAVC duct	1–5	PFA	1.5 g	0.4 g	GB/T 38591–2020 2020	
20	Cold water pipe	1–5	PFA	1.5 g	0.4 g	GB/T 38591–2020 2020	
21	Water tank	Roof	PFA	2.16 g	0.45 g	Shang 2021	
22	Water source	Well Water supply pipeline	Outdoors Outdoors	PGA PGV	0.15 g -	0.75 g -	FEMA 2022 -
23	Sewage pipe	1–5	PFA	1.2 g	0.5 g	GB/T 38591–2020 2020	
24	Outdoor drainage	Pump station Drainage pipeline	Outdoors Outdoors	PGA PGV	0.13 g -	0.6 g -	FEMA 2022 -
25	Communication device	1–5	PFA	2.16 g	0.45 g	Shang 2021	
26	Communication source	Central office Communication tower	Outdoors Outdoors	PGA PGA	0.13 g 0.57 g	0.55 g 0.55 g	FEMA 2022 RISN-TG041-2022 2022
27	Storage cabinet	1–5	PFA	0.6 g	0.6 g	Ning 2018	
28	Desk and chair	1–5	PFA	0.498 g	0.5 g	FEMA 2018b	
29	Blackboard	1–5	PIDR	0.01	0.3	FEMA 2018b	
30	Broadcasting speaker	1–5	PFA	2.5 g	0.5 g	FEMA 2018b	
31	Projection screen	1–5	PFA	2.5 g	0.5 g	FEMA 2018b	

Table 3 (continued)

No.	Component	Story distribution	EDP/IM	α_{dm}	β_{dm}	Ref.
32	Projector	1–5	PFA	1.1 g	0.32 g	FEMA 2018b
33	Office desk and chair	1–5	PFA	0.498 g	0.5 g	FEMA 2018b
34	File cabinet	1–5	PFA	0.498 g	0.5 g	FEMA 2018b
35	Computer	1–5	PFA	0.4 g	0.5 g	FEMA 2018b

Table 4 The selected ground motion records

Earthquake events	Year	Record station	M_w	Component	R_{ib}	$V_{s,30}$
Morgan Hill	1984	San Juan Bautista_24 Polk St	6.19	213	27.15	335.5
Chalfant Valley-02	1986	Convict Creek	6.19	90	29.35	382.12
Superstition Hills-02	1987	Plaster City	6.54	135	22.25	316.64
Loma Prieta	1989	Saratoga-Aloha Ave	6.93	90	7.58	380.89
Landers	1992	Barstow	7.28	0	34.86	370.08
Landers	1992	North Palm Springs	7.28	0	26.84	344.67
Big Bear-01	1992	Desert Hot Springs	6.46	90	39.52	359
Big Bear-01	1992	San Bernardino-2nd & Arrowhead	6.46	270	33.56	325.83
Kobe_Japan	1995	Kakogawa	6.9	0	22.5	312
Kocaeli_Turkey	1999	Goynuk	7.51	90	31.74	347.62
Parkfield-02_CA	2004	Coalinga-Fire Station 39	6	90	22.45	333.61
Darfield_New Zealand	2010	MAYC	7	E	33.54	342.7
Christchurch_New Zealand	2011	SBRC	6.2	E	43.88	263.2

Fig. 9 Comparison of mean response spectrum and design response spectrum

the ground motion characteristics are consistent for both the building and the site where the utility systems are distributed.

3.3 Immediate losses

Based on the EDPs obtained from thirteen ground motions, a matrix with 1000 sets of EDPs is established. Each set of parameters is sequentially extracted to simulate the damage states of stories and components. The damage state of each story is determined according to the discrimination criteria provided by Lv et al. (2006). Several publications (Ning 2018; FEMA 2018b; GB/T 38591–2020 2020; Shang 2021; Cong 2022; RISN-TG041-2022

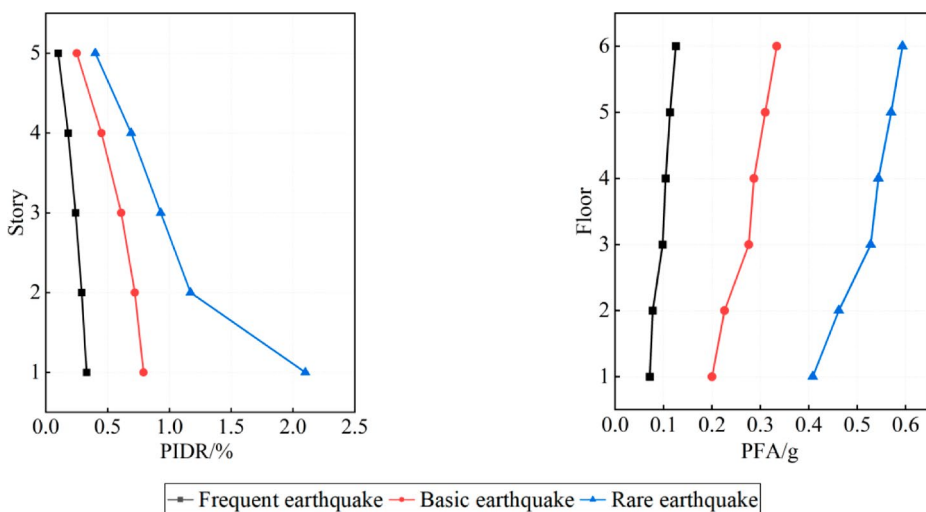


Fig. 10 Seismic responses of the teaching building

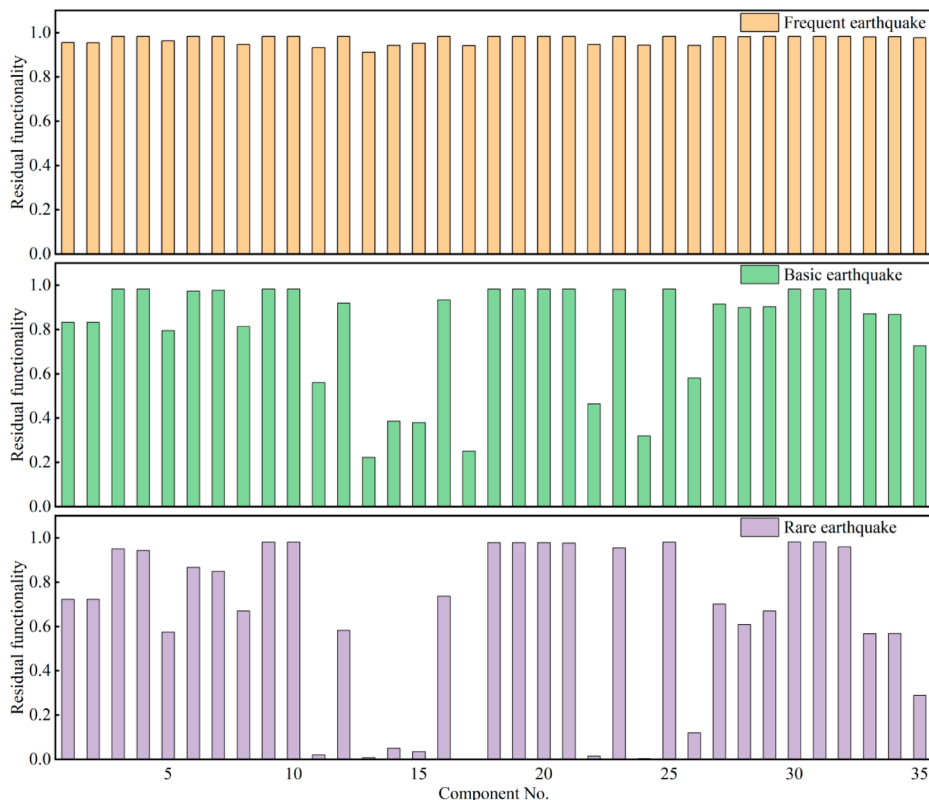
2022) provide abundant fragility curves for structural or nonstructural components. However, specific components related to the teaching function, like projectors and blackboards, lack clearly defined fragility curves in the available data. FEMA P-58-2 (FEMA 2018b) provides some vague fragility curves for unspecified items such as electronic equipment on walls and desktops, which can be used to represent the fragility of instructional components. It is worth noting that these fragility curves may not be specifically tailored to instructional components, but they serve as a valuable reference for evaluating the damage probability of the components. The fragility curves for the components considered are presented in Table 3. Based on Eq. (1), the probability of a component, excluding external utility pipelines, being in each damage state under a given EDP or IM is calculated. Some assumptions are made to consider the intra-story damage relevance as follows, and the representation of the damage state is expressed in a normalized manner.

If the slab is in DS1, then the ceiling is in DS1, the lamp is in DS1, the projector is in DS1, the HVAC duct fan is in DS1, and the HVAC duct is in DS1. If the infill wall is in DS1, then the blackboard is in DS1.

The residual functionality of the component in that damage state is obtained by sampling values from the triangular distribution it follows. Table 5 shows the triangular distribution parameters corresponding to the residual functionality for the ceiling under different damage states. The median parameter for each damage state is calculated using Eq. (5). When the ceiling is in DS0, the median parameter of the triangular distribution is 1, and the minimum parameter is 0.95. This accounts for the functional depreciation caused by service life and performance degradation. When the ceiling is in DS1, the median parameter is 0, and the maximum parameter is 0.15. This is because even when the ceiling is in the most severe damage state, there is still residual functionality, as DS1 signifies more than 50% of ceiling damage. After contemplating the descriptions of damage states from published literature (Ning 2018; FEMA 2018b; GB/T 38591–2020 2020; Shang 2021; Cong 2022; RISN-TG041-2022 2022), the suggested values for the triangular distribution parameters of residual functionality for all considered components are shown in Appendix I.

Table 5 The triangular distribution parameters of residual functionality for ceilings

Component	Parameter	Damage state			
		DS0	DS0.33	DS0.67	DS1
Ceiling	$Q_{r,\min}$	0.95	0.55	0.15	0
	$Q_{r,\text{med}}$	1	0.67	0.33	0
	$Q_{r,\max}$	1	0.85	0.55	0.15

**Fig. 11** Average residual functionality of components under different seismic intensity levels

After conducting 1,000 simulations, the average residual functionality of components of all stories is shown in Fig. 11. Observations reveal that the residual functionality gradually decreases as the seismic intensity increases. When subjected to frequent earthquakes, the residual functionality of components is generally above 0.9, sufficient to sustain educational activities without class suspension. For basic earthquakes, utility systems suffer significant shocks, leading to substantial functional degradation. For example, the functionality of the heating network drops to 0.251, indicating that in 1,000 simulation outcomes, the teaching building might fail to receive heating services in no more than 749 instances. This equates to a probabilistic assessment that the actual probability of the heating network failure during a basic earthquake would not exceed 74.9%. Displacement-sensitive components such as infill walls and stairs demonstrate notable performance deterioration, with their residual functionality decreasing approximately 20% as the inter-story drift ratio increases.

Components associated with the air conditioning system, including cooling equipment, air compressors, and air handling units, are more severely affected compared to infill walls and stairs. Under rare earthquakes, these components experience a significant decline, with residual functionality dropping even below 0.1. Due to their sensitivity to acceleration, seismic isolation techniques can be implemented to mitigate the transmission of seismic action to maintain functionality (Xu 2007; Xu et al. 2016 2017; Domenico and Ricciardi 2018; Gökçe et al. 2019; Chen and Xiong 2022). Desks and chairs, file cabinets, and computers that are used for teaching purposes also exhibit a notable trend of functional reduction. Securing or anchoring these items is a viable option to reduce their vulnerability. Infill walls experience a 27.7% decrease in functionality from basic to rare earthquakes. The damage or collapse of infill walls may jeopardize human safety and impair the building's insulation system, leading to a sharp drop in indoor temperature, particularly in cold regions. New systems have been developed to improve the earthquake resistance of exterior walls. The vertical functionality of the teaching building also suffers disruption. The stairs exhibit an average residual functionality of 0.671, with most simulations showing them in the second damage state. Notably, the first story displays the maximum PIDR, suggesting a more severe damage state and further reduced functionality. Aside from the communication network, which in some simulations still retains the possibility of providing communication services with an average residual functionality of 0.119, other utility systems, such as water, heating, and drainage networks, are basically nonfunctional. Figure 11 clearly identifies the components that impair building functionality. Effective pre-earthquake reinforcement measures can be adopted to strengthen these components to prevent significant functional losses and minimize interruptions to education in the event of a disaster. Additionally, this analysis provides a basis for developing recovery strategies, such as prioritizing the repair of components experiencing severe functional degradation to expedite the recovery of the teaching building.

Figure 12 depicts the average residual functionality of each story under different seismic intensity levels. The residual functionality exhibits a progressive upward trend across stories of the building. As presented in Fig. 10, the PIDR decreases with ascending stories, whereas the PFA escalates. The gradually increasing story functionality indicates that the functional losses for acceleration-sensitive components are less significant compared to the gains in displacement-sensitive components under these coupled effects. When encountering frequent earthquakes, minor component damage maintains story functionality above 0.932 across all stories, with functionality relevance yielding negligible impacts due to limited damage extent. For basic earthquakes, the functionality of each story significantly decreases, especially at the first story, which experiences a 53% reduction. Story functionality shows measurable reductions when functionality relevance is accounted for, with the magnitude of reduction increasing at higher stories. For example, story functionality decreases by 2.5% at the second story, and this reduction sharply escalates to 17.4% at the fifth story. This phenomenon reflects the dominant influence of displacement-sensitive stairs over acceleration-sensitive pipes (cold water pipes, sewage pipes, and caliducts) within the context of functionality relevance. As corroborated by Fig. 11, stairs exhibit considerably lower residual functionality of 0.814 compared to pipes with functionality exceeding 0.934 under basic earthquakes, confirming the critical role of stairs in vulnerability propagation. During rare earthquakes, the functionality of the first story plummets to 0.09 as utility services essentially cease. The inclusion of functionality relevance exacerbates story func-

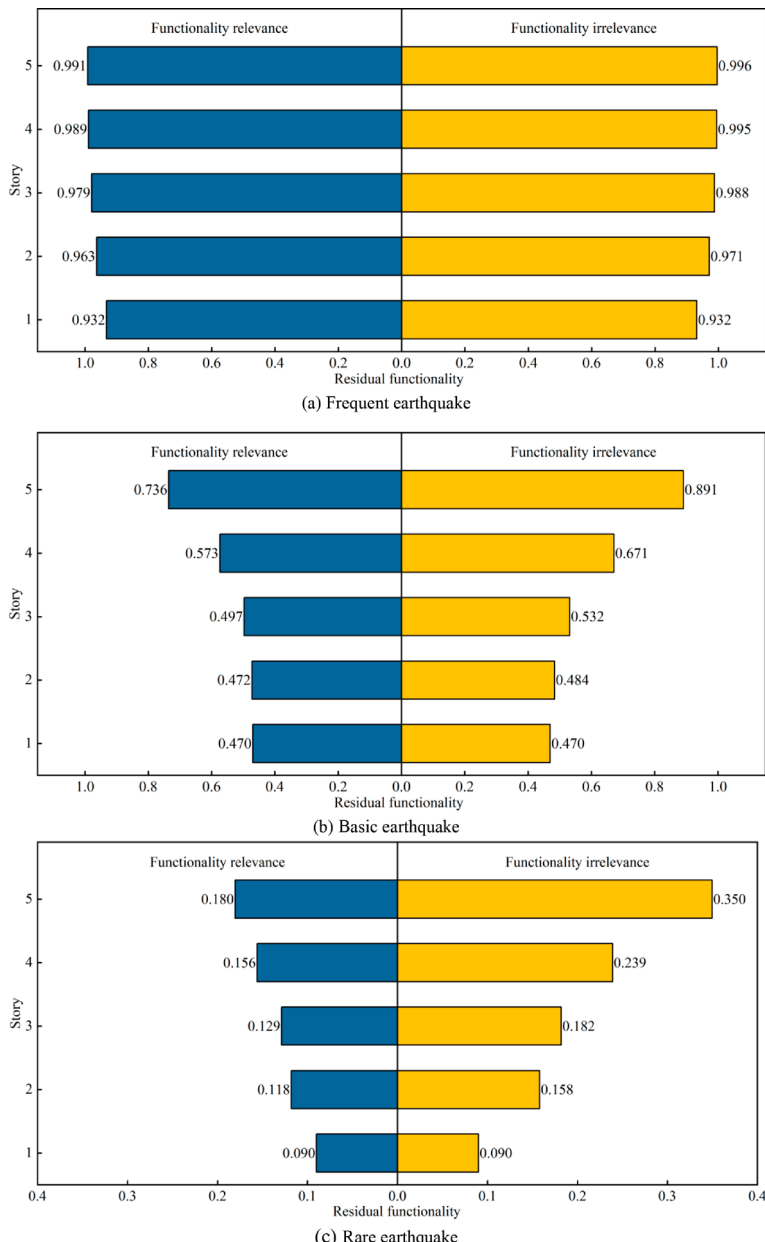


Fig. 12 Comparison of story functionality considering functionality relevance and functionality irrelevance

tionality more severely than under basic earthquakes, reaching up to a 48.6% reduction at the fifth story. This demonstrates that as seismic intensity increases, the consideration of functionality relevance exacerbates the detrimental effects on story functionality.

Figure 13 presents the distribution of immediate post-earthquake losses of the teaching building across 1,000 simulations under three seismic intensity levels. The repair cost ratio is calculated using Method A. The building replacement cost is determined as \$1,108,758 based on engineering specifications and current quotas. The analysis assumes an occupant density of 0.5 occupants/m² per story and an in-building rate of 0.98 (corresponding to class hours). The casualty rates under different damage states are obtained from RISNTG041-2022 (2022). Casualty severity levels 1–4 indicate an increase in the casualty severity, with weights of 1, 1, 1.5, and 2, respectively. Under frequent earthquakes, functional losses are minimal, with 911 simulations showing losses below 0.1 and an average of 0.0293. This aligns with real-world observations where minor seismic events rarely disrupt school operations, allowing educational activities to proceed normally. Repair costs under this intensity are equally modest, with 890 simulations exhibiting a repair cost ratio below 0.005 and an average of 0.0023. Casualty ratios are predominantly concentrated below 0.0019 (93.3% of simulations), including 564 simulations with zero casualties, yielding an overall average of 0.0004. In contrast, basic earthquakes reveal more pronounced impacts. Functional losses predominantly cluster within the range of 0.3556 to 0.6222, averaging 0.4505. Repair cost ratios show a broader distribution, spanning 0.00793 to 0.07324, with the majority concentrated between 0.014 and 0.035 and an average of 0.0247. Casualty ratios exhibit greater dispersion under this intensity, with nearly half of the results falling within the interval [0.00525, 0.00875] and an average of 0.0056. Rare earthquakes induce

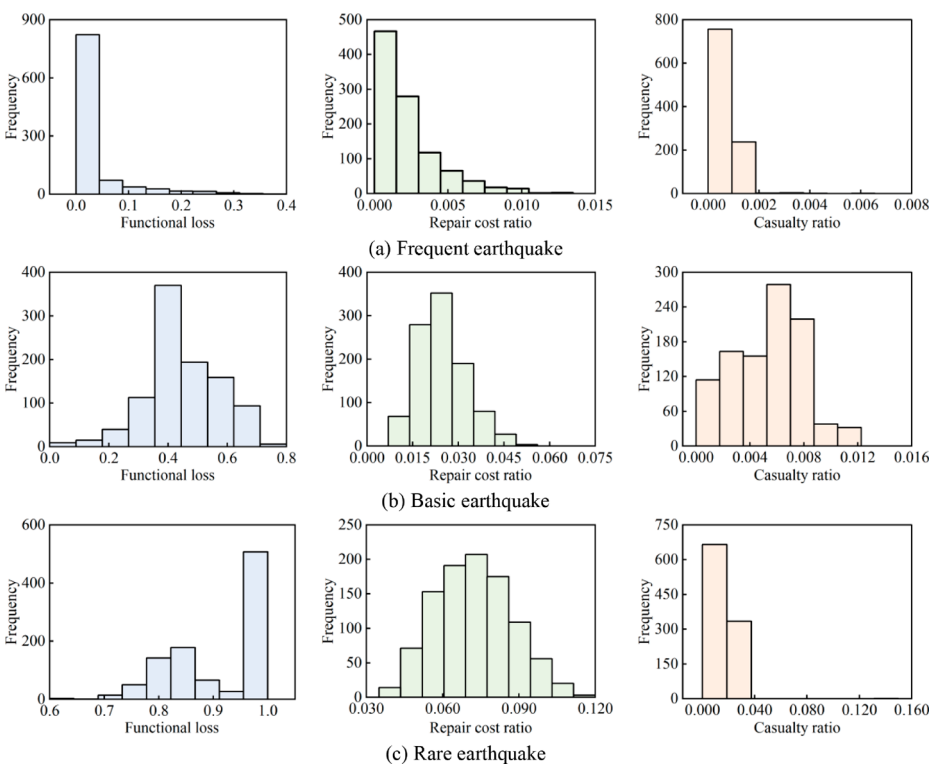


Fig. 13 Immediate post-earthquake losses under different seismic intensity levels

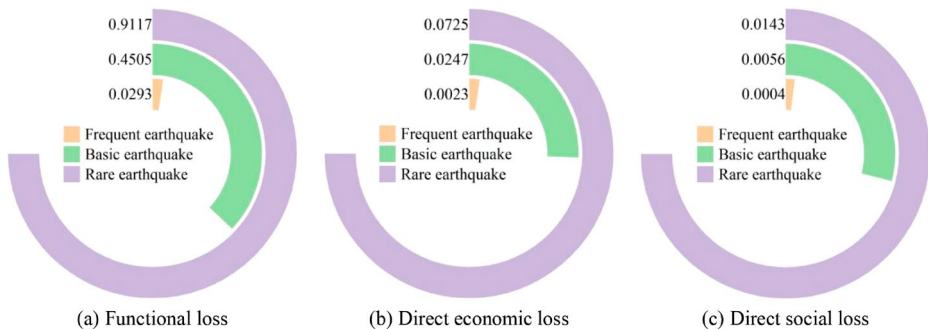


Fig. 14 Averages of immediate post-earthquake losses under different seismic intensity levels

catastrophic consequences. Functionality completely fails in 487 simulations, corresponding to scenarios where the first story sustains damage exceeding moderate damage thresholds. Repair cost ratios escalate to an average ratio of 0.0725, meeting the Two-Star Resilience Rating requirements specified in GB/T 38591–2020 (2020). Casualty ratios, predominantly below 0.0375, rise to an average of 0.0143.

The average values of immediate post-earthquake losses are summarized in Fig. 14. Among these losses, direct social losses (i.e., casualties) appear quantitatively minimal but carry profound societal implications. While the casualty ratio under rare earthquakes averages 0.0143—equivalent to approximately 1.4 casualties per 100 occupants—such outcomes remain ethically unacceptable despite their statistical representation. This assessment, however, is inherently tied to key assumptions: a 0.98 in-building rate (indicating densely populated classrooms) and predefined casualty severity weights. For example, if seismic events occurred during off-hours with sparse occupancy, the casualty ratio could decrease substantially. Direct economic losses, quantified through the repair cost ratio, remain within manageable thresholds across all scenarios. The repair cost ratio of 0.0725 under rare earthquakes aligns with Two-Star Resilience Rating requirements outlined in GB/T 38591–2020 (2020). Nevertheless, functional losses emerge as the most critical concern, which may not be significant in frequent earthquakes but can nearly lead to complete loss of functionality in rare earthquakes. This would result in a prolonged post-earthquake recovery period, significantly hindering the continuity of education. As the understanding of resilience deepens, the design paradigm is gradually shifting from the performance-based seismic design method to the resilience-based seismic design method. The latter aims to minimize post-earthquake losses, ensure rapid recovery, and reduce the adverse impact on social sustainability. The immediate post-earthquake losses evaluation method proposed in this study can serve as a cornerstone for the development of resilience-based seismic design.

4 Conclusion

This study presents a generalized method for evaluating immediate post-earthquake losses of buildings from engineering, economic, and social perspectives. The method is applied to a teaching building. Several valuable conclusions are as

- follows:
- (1) A new method is developed to evaluate the functional loss of buildings. This method incorporates a functional composition diagram, enabling inference from component functionality to story functionality. When aggregating from story functionality to building functionality, occupancy types, area, damage states of stories are considered.
 - (2) The intra-story damage relevance and the inter-story functionality relevance increase the vulnerability of buildings. The availability of external utility systems significantly impacts building functionality.
 - (3) The functional loss of components is influenced by the type of EDP or IM and its relative magnitude to the damage state threshold. A larger response or a smaller threshold will lead to significant functional loss. Two potential options to mitigate this are reducing seismic action transmitted to components or enhancing their resistance to earthquakes, which can be achieved through strategies such as isolation, anchoring, or developing new types of components with stronger resistance.
 - (4) Evaluating post-earthquake losses from the perspective of stories is more reasonable due to differences in the occupancy types of different stories. In addition to economic and social losses, post-earthquake functional loss also needs to be considered in building seismic design.

Appendix 1: Triangular distribution parameters of residual functionality

No.	Component	Parameter	Damage state						
			DS0	DS0.25	DS0.33	DS0.5	DS0.67	DS0.75	DS1
1	Beam	$Q_{r,\min}$	0.95	0.65	-	0.45	-	0.1	0
		$Q_{r,\text{med}}$	1	0.75	-	0.5	-	0.25	0
		$Q_{r,\max}$	1	0.95	-	0.65	-	0.45	0
2	Column	$Q_{r,\min}$	0.95	0.65	-	0.45	-	0.1	0
		$Q_{r,\text{med}}$	1	0.75	-	0.5	-	0.25	0
		$Q_{r,\max}$	1	0.95	-	0.65	-	0.45	0
3	Slab	$Q_{r,\min}$	0.95	-	-	0.3	-	-	0
		$Q_{r,\text{med}}$	1	-	-	0.5	-	-	0
		$Q_{r,\max}$	1	-	-	0.7	-	-	0
4	Curtain wall	$Q_{r,\min}$	0.95	-	0.45	-	0.1	-	0
		$Q_{r,\text{med}}$	1	-	0.67	-	0.33	-	0
		$Q_{r,\max}$	1	-	0.8	-	0.45	-	0.15
5	Infill wall	$Q_{r,\min}$	0.95	-	0.5	-	0.1	-	0
		$Q_{r,\text{med}}$	1	-	0.67	-	0.33	-	0
		$Q_{r,\max}$	1	-	0.95	-	0.5	-	0.15
6	Window and door	$Q_{r,\min}$	0.95	-	-	-	-	-	0
		$Q_{r,\text{med}}$	1	-	-	-	-	-	0
		$Q_{r,\max}$	1	-	-	-	-	-	0.15
7	Ceiling	$Q_{r,\min}$	0.95	-	0.55	-	0.15	-	0
		$Q_{r,\text{med}}$	1	-	0.67	-	0.33	-	0
		$Q_{r,\max}$	1	-	0.85	-	0.55	-	0.15

No.	Component	Parameter	Damage state						
			DS0	DS0.25	DS0.33	DS0.5	DS0.67	DS0.75	DS1
8	Stair	$Q_{r,\min}$	0.95	-	0.5	-	0.25	-	0
		$Q_{r,\text{med}}$	1	-	0.67	-	0.33	-	0
		$Q_{r,\max}$	1	-	0.9	-	0.5	-	0.15
9	Low-voltage switch	$Q_{r,\min}$	0.95	-	-	-	-	-	0
		$Q_{r,\text{med}}$	1	-	-	-	-	-	0
		$Q_{r,\max}$	1	-	-	-	-	-	0
10	Distributor	$Q_{r,\min}$	0.95	-	-	-	-	-	0
		$Q_{r,\text{med}}$	1	-	-	-	-	-	0
		$Q_{r,\max}$	1	-	-	-	-	-	0
11	Power source	$Q_{r,\min}$	0.95	0.6	-	0	-	0	0
		$Q_{r,\text{med}}$	1	0.75	-	0	-	0	0
		$Q_{r,\max}$	1	0.95	-	0	-	0	0
	Transmission and distribution line	$Q_{r,\min}$	0.95	0.6	-	0	-	0	0
		$Q_{r,\text{med}}$	1	0.75	-	0	-	0	0
		$Q_{r,\max}$	1	0.95	-	0	-	0	0
12	Lamp	$Q_{r,\min}$	0.95	-	-	-	-	-	0
		$Q_{r,\text{med}}$	1	-	-	-	-	-	0
		$Q_{r,\max}$	1	-	-	-	-	-	0
13	Cooling equipment	$Q_{r,\min}$	0.95	-	-	-	-	-	0
		$Q_{r,\text{med}}$	1	-	-	-	-	-	0
		$Q_{r,\max}$	1	-	-	-	-	-	0
14	Compressor	$Q_{r,\min}$	0.95	-	-	-	-	-	0
		$Q_{r,\text{med}}$	1	-	-	-	-	-	0
		$Q_{r,\max}$	1	-	-	-	-	-	0
15	Air handling unit	$Q_{r,\min}$	0.95	-	-	-	-	-	0
		$Q_{r,\text{med}}$	1	-	-	-	-	-	0
		$Q_{r,\max}$	1	-	-	-	-	-	0
16	Caliduct	$Q_{r,\min}$	0.95	-	-	0.35	-	-	0
		$Q_{r,\text{med}}$	1	-	-	0.5	-	-	0
		$Q_{r,\max}$	1	-	-	0.85	-	-	0.1
17	Heating source	$Q_{r,\min}$	0.95	0.6	-	0	-	0	0
		$Q_{r,\text{med}}$	1	0.75	-	0	-	0	0
		$Q_{r,\max}$	1	0.95	-	0	-	0	0
18	HVAC duct fan	$Q_{r,\min}$	0.95	-	-	0.4	-	-	0
		$Q_{r,\text{med}}$	1	-	-	0.5	-	-	0
		$Q_{r,\max}$	1	-	-	0.7	-	-	0
19	HAVC duct	$Q_{r,\min}$	0.95	-	-	0.4	-	-	0
		$Q_{r,\text{med}}$	1	-	-	0.5	-	-	0
		$Q_{r,\max}$	1	-	-	0.65	-	-	0
20	Cold water pipe	$Q_{r,\min}$	0.95	-	-	0.35	-	-	0
		$Q_{r,\text{med}}$	1	-	-	0.5	-	-	0
		$Q_{r,\max}$	1	-	-	0.85	-	-	0.1
21	Water tank	$Q_{r,\min}$	0.95	-	-	-	-	-	0
		$Q_{r,\text{med}}$	1	-	-	-	-	-	0
		$Q_{r,\max}$	1	-	-	-	-	-	0.1

No.	Component	Parameter	Damage state						
			DS0	DS0.25	DS0.33	DS0.5	DS0.67	DS0.75	DS1
22	Water source	$Q_{r,\min}$	0.95	0.6	-	0	-	0	0
		$Q_{r,\text{med}}$	1	0.75	-	0	-	0	0
		$Q_{r,\max}$	1	0.95	-	0	-	0	0
23	Sewage pipe	$Q_{r,\min}$	0.95	-	-	-	-	-	0
		$Q_{r,\text{med}}$	1	-	-	-	-	-	0
		$Q_{r,\max}$	1	-	-	-	-	-	0.1
24	Outdoor drainage	$Q_{r,\min}$	0.95	0.6	-	0	-	0	0
		$Q_{r,\text{med}}$	1	0.75	-	0	-	0	0
		$Q_{r,\max}$	1	0.95	-	0	-	0	0
25	Communication device	$Q_{r,\min}$	0.95	-	-	-	-	-	0
		$Q_{r,\text{med}}$	1	-	-	-	-	-	0
		$Q_{r,\max}$	1	-	-	-	-	-	0
26	Communication source	$Q_{r,\min}$	0.95	0.6	-	0	-	0	0
		$Q_{r,\text{med}}$	1	0.75	-	0	-	0	0
		$Q_{r,\max}$	1	0.95	-	0	-	0	0
26	Central office	$Q_{r,\min}$	0.95	0.6	-	0	-	0	0
		$Q_{r,\text{med}}$	1	0.75	-	0	-	0	0
		$Q_{r,\max}$	1	0.95	-	0	-	0	0
26	Communication tower	$Q_{r,\min}$	0.95	0.6	-	0	-	0	0
		$Q_{r,\text{med}}$	1	0.75	-	0	-	0	0
		$Q_{r,\max}$	1	0.95	-	0	-	0	0
27	Storage cabinet	$Q_{r,\min}$	0.95	-	-	-	-	-	0
		$Q_{r,\text{med}}$	1	-	-	-	-	-	0.2
		$Q_{r,\max}$	1	-	-	-	-	-	0.5
28	Desk and chair	$Q_{r,\min}$	0.95	-	-	-	-	-	0
		$Q_{r,\text{med}}$	1	-	-	-	-	-	0.2
		$Q_{r,\max}$	1	-	-	-	-	-	0.5
29	Blackboard	$Q_{r,\min}$	0.95	-	-	-	-	-	0
		$Q_{r,\text{med}}$	1	-	-	-	-	-	0.2
		$Q_{r,\max}$	1	-	-	-	-	-	0.5
30	Broadcasting speaker	$Q_{r,\min}$	0.95	-	-	-	-	-	0
		$Q_{r,\text{med}}$	1	-	-	-	-	-	0
		$Q_{r,\max}$	1	-	-	-	-	-	0
31	Projection screen	$Q_{r,\min}$	0.95	-	-	-	-	-	0
		$Q_{r,\text{med}}$	1	-	-	-	-	-	0
		$Q_{r,\max}$	1	-	-	-	-	-	0.1
32	Projector	$Q_{r,\min}$	0.95	-	-	-	-	-	0
		$Q_{r,\text{med}}$	1	-	-	-	-	-	0
		$Q_{r,\max}$	1	-	-	-	-	-	0
33	Office desk and chair	$Q_{r,\min}$	0.95	-	-	-	-	-	0
		$Q_{r,\text{med}}$	1	-	-	-	-	-	0.2
		$Q_{r,\max}$	1	-	-	-	-	-	0.5
34	File cabinet	$Q_{r,\min}$	0.95	-	-	-	-	-	0
		$Q_{r,\text{med}}$	1	-	-	-	-	-	0.2
		$Q_{r,\max}$	1	-	-	-	-	-	0.5
35	Computer	$Q_{r,\min}$	0.95	-	-	-	-	-	0
		$Q_{r,\text{med}}$	1	-	-	-	-	-	0
		$Q_{r,\max}$	1	-	-	-	-	-	0

Author contributions Shuang Li: Conceptualization, Funding acquisition, Methodology, Supervision, Writing - review & editing; Binbin Hu: Formal analysis, Conceptualization, Methodology, Investigation, Soft-

ware, Writing - original draft preparation; Changhai Zhai: Resources, Writing - review & editing; Paloma Pineda: Writing - review & editing.

Funding This work was supported by the National Natural Science Foundation of China under Grant No. 52478508 and National Key Research and Development Program of China under Grant No. 2023YFC3805003. The supports are greatly appreciated by the authors.

Data availability The datasets generated during the current study are available from the corresponding author on reasonable request.

Declarations

Competing interests The authors have no relevant financial or non-financial interests to disclose.

References

- Almufti I, Willford M (2013) REDiTTM rating system: resilience-based earthquake design initiative for the next generation of buildings. Arup, London
- Anwar GA, Dong Y, Ouyang M (2023) Systems thinking approach to community buildings resilience considering utility networks, interactions, and access to essential facilities. *Bull Earthq Eng* 21:633–661
- ATC, Applied Technology Council (1985) ATC-13 Earthquake damage evaluation data for California. California
- Bruneau M, Chang SE, Eguchi RT (2003) A framework to quantitatively assess and enhance the seismic resilience of communities. *Earthq Spectra* 19(4):733–752
- Chen X, Xiong J (2022) Seismic resilient design with base isolation device using friction pendulum bearing and viscous damper. *Soil Dyn Earthq Eng* 153:107073
- Cong Y (2022) Study on Multi-level Function Loss and Seismic Resilience Assessment Method of Urban Complex. Dissertation, Dalian University of Technology (in Chinese)
- Cook DT, Liel AB, DeBock DJ, Haselton CB (2021) Benchmarking FEMA P-58 repair costs and unsafe placards for the Northridge Earthquake: implications for performance-based earthquake engineering. *Int J Disast Risk Reduct* 56:102117
- D'Ayala DF, Paganoni S (2011) Assessment and analysis of damage in L'Aquila historic city centre after 6th April 2009. *Bull Earthq Eng* 9:81–104
- Dhakal RP, Mander JB (2005) Probabilistic risk assessment methodology framework for natural hazards. Report submitted to Institute of Geological and Nuclear Science(IGNS). Christchurch, New Zealand: Department of Civil Engineering, University of Canterbury
- Domenico DD, Ricciardi G (2018) An enhanced base isolation system equipped with optimal tuned mass damper inerter (TMDI). *Earthq Eng Struct Dyn* 47:1169–1192
- Dong Y, Frangopol DM (2016) Performance-based seismic assessment of conventional and base-isolated steel buildings including environmental impact and resilience. *Earthq Eng Struct Dyn* 45(5):739–756
- FEMA, Federal Emergency Management Agency (2018a) FEMA P-58-1: seismic performance assessment of buildings, volume 1—methodology. Washington, DC
- FEMA, Federal Emergency Management Agency (2018b) FEMA P-58-2: seismic performance assessment of buildings, volume 2 – implementation guide. Washington, DC
- FEMA, Federal Emergency Management Agency (2022) HAZUS-MH5.1 Technical Manual. Federal Emergency Management Agency. Washington, DC
- GB 50011–2010 (2010) Code for seismic design of buildings. Beijing (in Chinese)
- GB 50137–2011 (2011) Code for classification of urban land use and planning standards of development land. Beijing (in Chinese)
- GB/T 38591–2020 (2020) Standard for seismic resilience assessment of buildings. Beijing (in Chinese)
- Gehl P, Matsushima S, Masuda S (2021) Investigation of damage to the water network of Uki City from the 2016 Kumamoto earthquake: derivation of damage functions and construction of infrastructure loss scenarios. *Bull Earthq Eng* 19:685–711
- Gökçe T, Yüksel E, Orakdögen E (2019) Seismic performance enhancement of high-voltage post insulators by a polyurethane spring isolation device. *Bull Earthq Eng* 17:1739–1762
- González C, Niño M, Jaimes MA (2020) Event-based assessment of seismic resilience in Mexican school buildings. *Bull Earthq Eng* 18:6313–6336

- Hassan EM, Hussam M (2018) A framework for estimating immediate interdependent functionality reduction of a steel hospital following a seismic event. *Eng Struct* 168:669–683
- Jiang H, Bu H, He L (2022) A new method for function-loss based seismic resilience assessment of buildings. *Eng Struct* 266:114613
- Kamata H, Seto S, Suppasri A, Sasaki H, Egawa S, Imamura F (2022) A study on hypothermia and associated countermeasures in tsunami disasters: a case study of Miyagi Prefecture during the 2011 great East Japan earthquake. *Int J Disast Risk Reduct* 81:103253
- Kitayama S, Moncayo M, Athanasiou A (2023) Inspection and repair considerations for downtime assessment of seismically isolated buildings. *Soil Dyn Earthq Eng* 164:107618
- Li L, Richard A, Boston M, Elwood K, Hutt CM (2023) Post-disaster functional recovery of the built environment: a systematic review and directions for future research. *Int J Disast Risk Reduct* 95:103899
- Li S, Hu B, Hou Z, Zhai C (2024) A novel method for post-earthquake functional evaluation of city building portfolios. *J Build Eng* 89:109269
- Li Y, Zhang Z, Xin D (2021) A Composite Catalog of Damaging Earthquakes for Mainland China. *Seismol Res Lett* 92(6):3767–3777
- Lu X, Chen A (2022) Quantitative evaluation and improvement of seismic resilience of a tall frame shear wall structure. *Struct Des Tall Spec Build* 31(1):e1899
- Lv D, Li X, Wang G (2006) Global seismic fragility analysis of structures based on reliability and performance. *J Natural Disasters* 15(02):107–114. (in Chinese)
- Martínez-Cuevas S, Gaspar-Escribano JM (2016) Reassessment of intensity estimates from vulnerability and damage distributions: the 2011 Lorca earthquake. *Bull Earthq Eng* 14:2679–2703
- McKenna F, Fenves GL, Scott MH, Jeremic B (2000) Open system for earthquake engineering Simulation. Pacific Earthquake Engineering Research Center: University of California, Berkeley, California
- Melani A, Khare RK, Dhakal RP, Mander JB (2016) Seismic risk assessment of low rise RC frame structure. *Structure* 5:13–22
- Menna C, Felicioni L, Negro P, Lupišek A, Romano E, Prota A, Hájek P (2022) Review of methods for the combined assessment of seismic resilience and energy efficiency towards sustainable retrofitting of existing European buildings. *Sust Cities Soc* 77:103556
- Ning X (2018) Research on Evaluation Methodology of Seismic Safety and Resilience for Significant Buildings. Dissertation, Institute of Engineering Mechanics, China Earthquake Administration (in Chinese)
- Porter K, Ramer K (2012) Estimating earthquake-induced failure probability and downtime of critical facilities. *J Bus Contin Emer Plan* 5:352–364
- Qu Z, He S, Fu H (2020) Computational Evaluation of the Functional Loss and Recovery of Individual Building. *J Perform Constr Facil* 34(3):04020042
- RISN-TG041-2022 (2022) Guideline for evaluation of seismic resilience assessment of urban engineering systems. Beijing (in Chinese)
- Sagbas G, Garjan RS, Sarikaya K, Deniz D (2024) Field reconnaissance on seismic performance and functionality of Turkish industrial facilities affected by the 2023 Kahramanmaraş earthquake sequence. *Bull Earthq Eng* 22:227–254
- Shang Q, Wang T, Li J (2020) Seismic assessment of emergency departments based on the state tree method. *Struct Saf* 85:101944
- Shang Q (2021) Research on seismic resilience assessment method of hospital systems. Dissertation, Institute of Engineering Mechanics, China Earthquake Administration (in Chinese)
- Song R, Li Y, De Lindt W V (2016) Loss estimation of steel buildings to earthquake mainshock - aftershock sequences. *Struct Saf* 61:1–11
- Tang Y, Li S, Zhai C (2023) A belief rule-base approach to the assessment and improvement of seismic resilience of high-speed railway station buildings. *Soil Dyn Earthq Eng* 106:107680
- Terzic V, Villanueva PK (2021) Method for probabilistic evaluation of post-earthquake functionality of building systems. *Eng Struct* 241:112370
- Terzic V, Villanueva PK, Saldana D, Yoo DY (2021) Framework for modelling post-earthquake functional recovery of buildings. *Eng Struct* 246:113074
- Tesfamariam S, Goda K (2015) Loss estimation for non-ductile reinforced concrete building in Victoria, British Columbia, Canada: effects of mega-thrust Mw9-class subduction earthquakes and aftershocks. *Earthq Eng Struct Dyn* 44:2303–2320
- United Nations (2015) Sendai framework for disaster risk reduction 2015–2030. Geneva
- USCR, United States Resiliency Council (2017) United States Resiliency Council rating system implementation manual. California
- Wen W, Zhang M, Zhai C, Liu W (2019) Resilience loss factor for evaluation and design considering the effects of aftershocks. *Soil Dyn Earthq Eng* 116:43–49
- Xu Z (2007) Earthquake mitigation study on viscoelastic dampers for reinforced concrete structures. *J Vib Control* 13(1):29–45

- Xu Z, Liao Y, Ge T, Xu C (2016) Experimental and theoretical study on viscoelastic dampers with different matrix rubbers. *J Eng Mech* 142(8):04016051
- Xu Z, Gai P, Zhao H, Huang X, Lu L (2017) Experimental and theoretical study on a building structure controlled by multi-dimensional earthquake isolation and mitigation devices. *Nonlinear Dyn* 89(1):723–740
- Zhai C, Yue Q, Xie L (2024) Evaluation and construction of seismic resilient cities. *J Build Struct* 45(05):1–13. (in Chinese)
- Zhou YG, Xia P, Ling DS, Chen YM (2020) A liquefaction case study of gently sloping gravelly soil deposits in the near-fault region of the 2008 Mw7.9 Wenchuan earthquake. *Bull Earthq Eng* 18:6181–6201

Publisher's Note Springer Nature remains neutral with regard to jurisdictional claims in published maps and institutional affiliations.

Springer Nature or its licensor (e.g. a society or other partner) holds exclusive rights to this article under a publishing agreement with the author(s) or other rightsholder(s); author self-archiving of the accepted manuscript version of this article is solely governed by the terms of such publishing agreement and applicable law.